# Gas-Phase Reactions of Protonated Tryptophan†

Hadi Lioe* and Richard A. J. O'Hair
School of Chemistry, University of Melbourne, Melbourne, Victoria, Australia

Gavin E. Reid
Joint Proteomics Laboratory, The Ludwig Institute for Cancer Research and the Walter and Eliza Hall Institute of Medical Research, Royal Melbourne Hospital, Parkville, Victoria, Australia

The gas phase reactions of protonated tryptophan have been examined in a quadrupole ion trap using a combination of collision induced dissociation, hydrogen–deuterium exchange, regiospecific deuterium labeling and molecular orbital calculations (at the B3LYP/6-31G* level of theory). The loss of ammonia from protonated tryptophan is observed as the primary fragmentation pathway, with concomitant formation of a $[M + H - NH_3]^+$ ion by nucleophilic attack from the C3 position of the indole side chain. Hydrogen–deuterium exchange and regiospecific deuterium labeling reveals that scrambling of protons in the C2 and C4 positions of the indole ring, via intramolecular proton transfer from the thermodynamically preferred site of protonation at the amino nitrogen, precedes ammonia loss. Molecular orbital calculations have been employed to demonstrate that the activation barriers to intramolecular proton transfer are lower than that for $NH_3$ loss. (J Am Soc Mass Spectrom 2004, 15, 65–76) © 2004 American Society for Mass Spectrometry

Understanding the fragmentation reactions of protonated amino acids is not only important from an analytical perspective for diagnosis of inherited disorders of metabolism [1], and for automated interpretation and prediction of electrospray tandem mass spectra (ESI/MS/MS) [2], but also as models for developing the tools and concepts used to understand the mechanisms for the fragmentation mechanisms of protonated peptides (For studies on the mechanism of the fragmentation reactions of protonated amino acids see reference [3]). Simple aliphatic amino acids fragment via the loss of the combined elements of $H_2O$ and CO. Harrison and Yalcin have provided strong evidence for involvement of "mobile" protons in this fragmentation pathway by showing that the $[M + D]^+$ ions of valine and leucine undergo complete H/D scrambling prior to fragmentation [4]. This is consistent with the mechanism shown in Path (A) of Scheme **1** in which the thermodynamically favored protonated Form **A** undergoes scrambling via intramolecular proton transfer, via TS1, to the CO protonated Isomer **B**, prior to fragmentation induced by intramolecular proton transfer via TS2 or TS3 to the OH protonated Isomer **C**. These experimental observations are entirely consistent with two recent independent high level ab initio calculations on protonated glycine, which show that the relative activation energies for the various intramolecular proton transfer processes follow the order: E(TS1) < E(TS2) < E(TS3) [5].

When a protonated amino acid contains a functional group on its side chain, other fragmentation channels may be observed, such as the loss of ammonia from the N-terminus [6] or the loss of a small molecule such as water [7] or ammonia [8] from the side chain. For example, the fragmentation of cysteine and methionine exhibit ammonia loss [Path (B) in Scheme **1**] [6] that competes with loss of the combined elements of $[H_2O + CO]$ [Path (A) in Scheme **1**]. This fragmentation pathway involves a neighboring group process in which the sulphur atom of the sulfhydryl group or thioether group acts as an intramolecular nucleophile to induce ammonia loss via the transition state TS4 to form the product ion **D**. The fact that these competing fragmentation pathways are both observed under low energy CID is supported by ab initio calculations in protonated cysteine which showed that the transition states for fragmentation via Paths (A) and (B) (TS2 and TS4, respectively) have similar energies [6a].

Each of these results is entirely consistent with the two major concepts used to explain the mechanisms of peptide ion fragmentation reactions, i.e, the mobile proton model [9] and the role of neighboring groups to

Published online November 14, 2003

Address reprint requests to Associate Professor Richard A. J. O'Hair: Phone: +61 3 8344-6490; FAX: +61 3 9347-5180; E-mail: rohair@unimelb.edu.au; Dr. Gavin E. Reid: Phone: +61 3 9341-3155; FAX: +61 3 9341-3192; E-mail: gavin.reid@ludwig.edu.au.

*Also at Joint Proteomics Laboratory, the Ludwig Institute for Cancer Research and the Walter and Eliza Hall Institute of Medical Research, Royal Melbourne Hospital.

†This paper is Part 37 of the Series "Gas Phase Ion Chemistry of Biomolecules."


1044-0305/04/$30.00
doi:10.1067/j.jasms.2003.09.011

Received August 7, 2003
Revised September 23, 2003
Accepted September 24, 2003

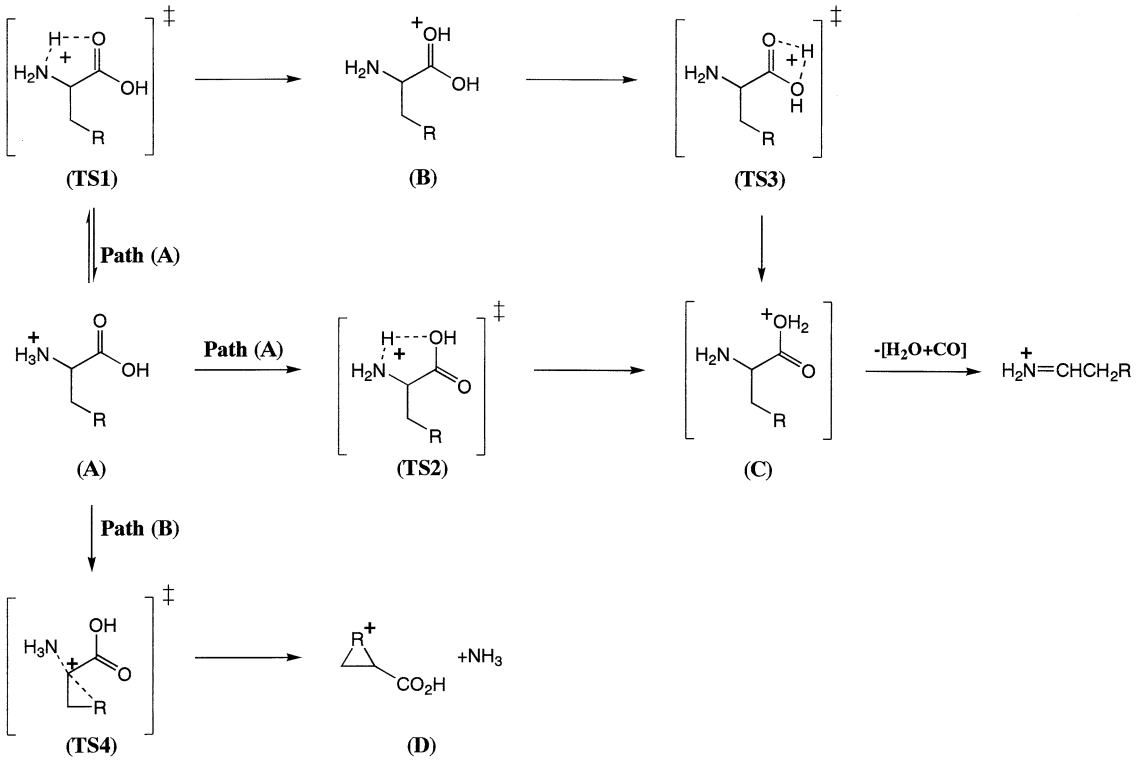


**Scheme 1**

help facilitate cleavage reactions [10] and support the generally accepted idea that under low energy CID conditions, the fragmentation reactions of protonated amino acids and peptides tend to be charge directed [10].

Although the protonated amino acids that readily lose ammonia have been established from previous CI/MS [3a], desorption MS [3b, c], FAB MS/MS [3d] and ESI MS/MS [3e] studies, the mechanisms for some of these losses remain obscure or in contention. For example, two different mechanistic proposals have been described for the loss of ammonia from protonated Tryptophan **E** (note the numbering of the indole ring system which will be used throughout). In the first, Prokai et al. used AM1 semiempirical calculations to suggest the mechanism shown in Scheme **2** for the loss of the N-terminus from a fixed charge derivative of tryptophan, via cyclization by nucleophilic attack from the C2 position of the indole ring to form **F**, followed by ring expansion to give **G**, driven by the stability of the final ion [11]. More recently, Rogalewicz et al. have used deuterium labeling and MS/MS in a triple quadrupole mass spectrometer to probe the gas-phase reactions of protonated tryptophan [3e]. They found that ammonia is lost exclusively and that when all the labile hydrogens (NH and OH) are replaced by deuterium, gas-phase hydrogen–deuterium scrambling occurs with subsequent loss of $ND_3$, $ND_2H$, and $NHD_2$. To rationalize this scrambling, they suggested that tryptophan is initially protonated on the nitrogen atom of the indole ring (**H** in Scheme **3**) and that this species isomerizes via a series of 1,2-hydride shifts around the indole ring to give **I**, which then undergoes ammonia loss via nucleophilic attack from the C4 position of the indole ring to form **J**.

Note that a number of alternative mechanistic possibilities may be proposed to explain the loss of ammonia from protonated tryptophan. For example, the spirocyclopropane derivative **K**, formed via nucleophilic attack from the C3 position of the indole ring, or the tricyclic product ion derivatives **L** and **M**, formed via nucleophilic attack from the C8 and C9 positions of the indole ring, respectively, could all be considered as potential products. While species related to **L** and **M** have not been described previously, **K** is not without precedence in the literature. For example, the condensed phase isomerization of a tryptophan analogue has been proposed to occur via an intermediate having the structure of **K** [12]. Furthermore, a related spirocyclopropane product ion formed by the loss of ammonia from protonated tyrosine has been proposed by Harrison and coworkers [3d], and has been supported by theoretical calculations [12a].

The scrambling observed during the loss of $NH_3$ from deuterium-labeled tryptophan could also be explained via alternative mechanisms. For example, direct intramolecular proton transfer from the protonated amino group to either the C2 or C4 positions of the indole ring could produce the observed losses. There is convincing evidence that a related mechanism involving scrambling of the C4 position of the indole ring operates under condensed phase photolysis conditions

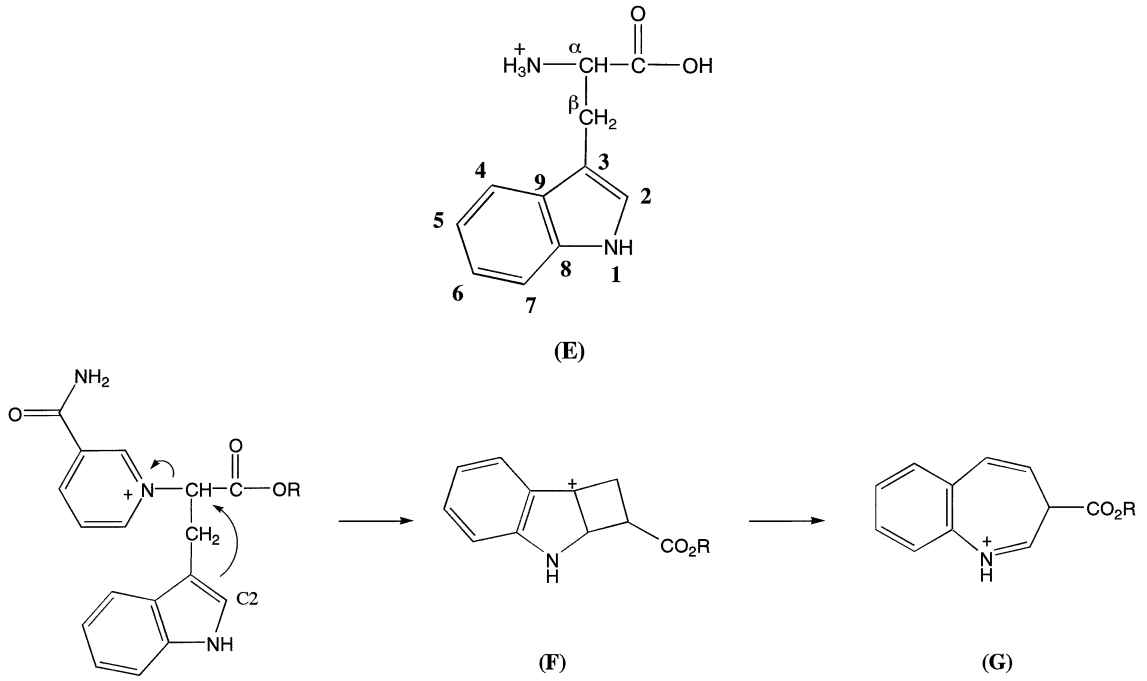


**Scheme 2**

[13]. Therefore, in order to resolve the issues discussed above, we examine in this paper the mechanisms for deuterium scrambling and ammonia loss from protonated tryptophan and related tryptophan species, using a combination of multistage tandem mass spectrometry experiments, hydrogen–deuterium exchange, regiospecific deuterium labeling, and molecular orbital calculations.

## Experimental

### *Materials*

Tryptophan and monodeuterated methanol ($CH_3OD$) were purchased from Aldrich (Milwaukee, WI). Tryptophan O-methyl ester, tryptophanylglycine, and glycyltryptophan were obtained from BACHEM (Bubendorf, Switzerland). Methanol (ChromAR grade) was purchased from Mallinkrodt (Melbourne, Australia). Deuterium oxide ($D_2O$) was obtained from Cambridge Isotope Laboratories (Andover, MA). Acetic acid was obtained from Merck (Darmstadt, Germany). Sodium deuteroxide was purchased from ICN Biomedicals (Cambridge, MA). Tryptophanyl-glycine O-methyl ester was synthesized using a method described previously [7a].

### *Mass Spectrometry*

Protonated tryptophan derivatives $[M + H]^+$ ions were formed via electrospray ionization (ESI) on a Finnigan model LCQ-deca (San Jose, CA) quadrupole ion trap mass spectrometer. Samples, (0.1 mg/mL) dissolved in 50% $CH_3OH$/50% $H_2O$ containing 0.1 M acetic acid, 50% $CH_3OH$/50% $H_2O$, or 50% $CH_3OD$/50% $D_2O$ were introduced to the mass spectrometer at 2 $\mu$L/min. The spray voltage was set at 4.5 kV. Nitrogen sheath gas was supplied at 25 psi. The heated capillary temperature was 250 °C. MS/MS experiments were performed on mass-selected ions in the quadrupole ion trap mass spectrometer using standard isolation and excitation procedures.

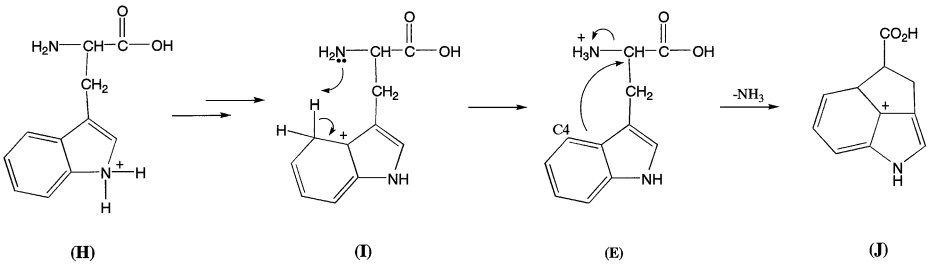


**Scheme 3**

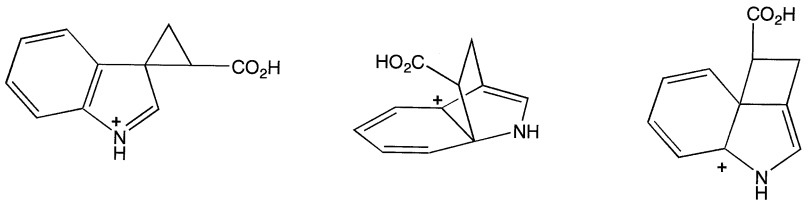


(K) (L) (M)

### ($N^{\alpha}$,$N^{\alpha}$,O,1-$^2H_4$) Tryptophan

($^2H_4$)-labeled tryptophan (all labile hydrogen, NH and OH exchanged) was prepared by dissolving the sample (0.1 mg/mL) in 50% $CH_3OD$/50% $D_2O$. $[M + D]^+$ ions were introduced to the mass spectrometer under the same conditions as described above, with the addition of an auxiliary gas (15, arbitrary units) to reduce deuterium back exchange during electrospray sample introduction.

### Regiospecific Deuterium Labeling of Tryptophan

Three different regiospecific deuterium labeled tryptophan species were prepared.

*(4-$^2H$) tryptophan.* Regiospecific hydrogen–deuterium exchange at the C4 indole position was carried out by intramolecular excited-state proton transfer according to the method of Saito et al. [13a]. Briefly, a solution of 10 mM tryptophan in $D_2O$ in an NMR tube was irradiated with pyrex-filtered high-pressure mercury lamp (Hanovia, 450W) for 3 h. The progress of the H/D exchange was monitored using 400-MHz $^1H$ NMR. The product was diluted to 0.1 mg/mL in 50% $CH_3OH$/50% $H_2O$ for MS analysis.

*($\alpha$,2-$^2H_2$) tryptophan.* The high temperature and pressure method of Griffiths et al. [14] was employed to perform regiospecific hydrogen–deuterium exchange at the C2 position of the indole ring. Ten mg of tryptophan was dissolved in 1.0 mL of $D_2O$ in a medium-walled pyrex glass vessel (10 mm i.d. and 12 mm o.d.) and the pD of the solution was adjusted to approximately 7.00 using NaOD. The tube was then flame sealed and heated at 145 °C for 5 days. For NMR analysis, the supernatant of the product was made up into a 10 mM solution in $D_2O$. For MS analysis, a 0.1mg/mL solution of the supernatant of the product was made up in 50% $CH_3OH$/50% $H_2O$. In addition to deuterium labeling at the C2 position, the $\alpha$-CH is also exchanged using this method. This was confirmed here by $^1H$ NMR. Note that the $C^{\alpha}$ deuterium is not expected to participate in the proton transfer process and simply adds a mass of 1Da to the ion.

*($N^{\alpha}$,$N^{\alpha}$,O,$\alpha$,1,2,4-$^2H_7$) tryptophan.* ($N^{\alpha}$,$N^{\alpha}$,O,$\alpha$,1,2,4-$^2H_7$) tryptophan was synthesized using a combination of both regiospecific deuterium labeling and hydrogen–deuterium exchange. A 10 mM solution of ($\alpha$,2-$^2H_2$) tryptophan in $D_2O$, prepared as described above, was irradiated in an NMR tube with pyrex-filtered high-pressure mercury lamp (Hanovia, 450W) for 10.5 h. The progress of the reaction was monitored using $^1H$ NMR. The product was then diluted to 0.1 mg/mL in 50% $CH_3OD$/50% $D_2O$ prior to MS analysis. An auxiliary gas (15, arbitrary unit) was also added to reduce deuterium back exchange during electrospray sample introduction.

### Computational Methods

Structures of minima and transition states were optimized at the B3LYP level of theory with the standard 6-31G* basis set [15] using the GAMESS [16] and GAUSSIAN 98 [17] molecular modeling packages. All optimized structures were subjected to vibrational frequency analysis and visualized using the computer package MOLDEN [18] to determine the nature of the stationary points. Energies were corrected for zero-point vibrations scaled by 0.9806 [19]. Intrinsic reaction coordinate (IRC) runs were performed on each transition state, followed by geometry optimizations to check that they connected to the appropriate reactant and product ion minima.

### Supplementary Materials

Complete structural details and lists of vibrational frequencies for each B3LYP/6-31G* optimized structure and $^1H$ NMR spectra of regiospecific deuterium labeled tryptophan derivatives are available from the authors upon request.

## Results and Discussion

### $NH_3$ Loss from the $[M + H]^+$ ions of Trp-X (where X = OH, $OCH_3$ and $NHCH_2CO_2H$)

Under low energy ion trap CID MS/MS conditions, the $[M + H]^+$ ions of tryptophan (*m/z* 205), tryptophan O-methyl ester (*m/z* 219), tryptophanyl-glycine (*m/z* 262), and tryptophanyl-glycine O-methyl ester (*m/z* 276) were all found to fragment via the exclusive loss of ammonia (shown in Figure 1 for protonated tryptophan). For protonated tryptophan, the combined loss of water and CO was only observed as a very low relative

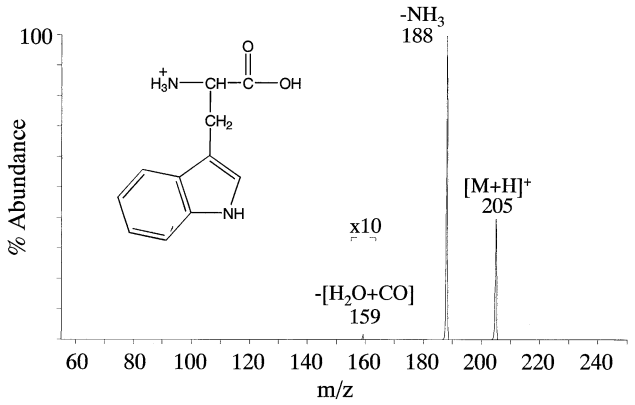


**Figure 1**. CID MS/MS spectrum of the $[M + H]^+$ ion of tryptophan.

abundance product. When dissolved in a solution of $CH_3OD/D_2O$, ESI/MS of tryptophan (*m/z* 210) indicated that only the labile hydrogens (NH and OH) had been exchanged for deuterium (data not shown). This is consistent with several NMR studies which have shown that the aromatic indole C–H hydrogens only exchange in the presence of strong acids such as trifluoroacetic acid (the relative rates of indole hydrogen exchange are: H2 > H5 ⩾ H6 > H4 ≈ H7) [20]. When the fully deuterated $[M + D]^+$ ion was subjected to CID, scrambling of the deuterons to give loss of $ND_3$, $ND_2H$, and $NH_2D$ in the ratio 2:4:1 was observed (Figure 2a), in accord with the previous results of Rogalewicz et al. [3e]. Thus, H/D scrambling occurs in the gas phase via intramolecular proton transfer. The fact that scrambling is observed for the $NH_3$ loss product ion indicates that intramolecular proton transfer is more energetically favorable than loss of $NH_3$. We have therefore used molecular orbital calculations to determine the possible pathways and relative energies for intramolecular proton transfer of tryptophan compared with that for $NH_3$ loss.

## *Computational Studies on the Site of Protonation of Tryptophan*

An examination of the literature reveals that there has been only one previous theoretical study on the protonation of tryptophan. Maksic and Kovacevic calculated the proton affinity of tryptophan at the MP2(fc)/6-311+G**//HF/6-31G* level of theory and found it to be 220.7 kcal/mol [21], which is in reasonable agreement with a recent experimental determination of 221.6 kcal/mol [22]. In their study, Maksic and Kovacevic also predicted that the amino nitrogen is the most favorable site of protonation for tryptophan. However, Rogalewicz et al. [3e] suggested that because of the high proton affinity of tryptophan, the most stable site of protonation is the indole nitrogen of the side chain of

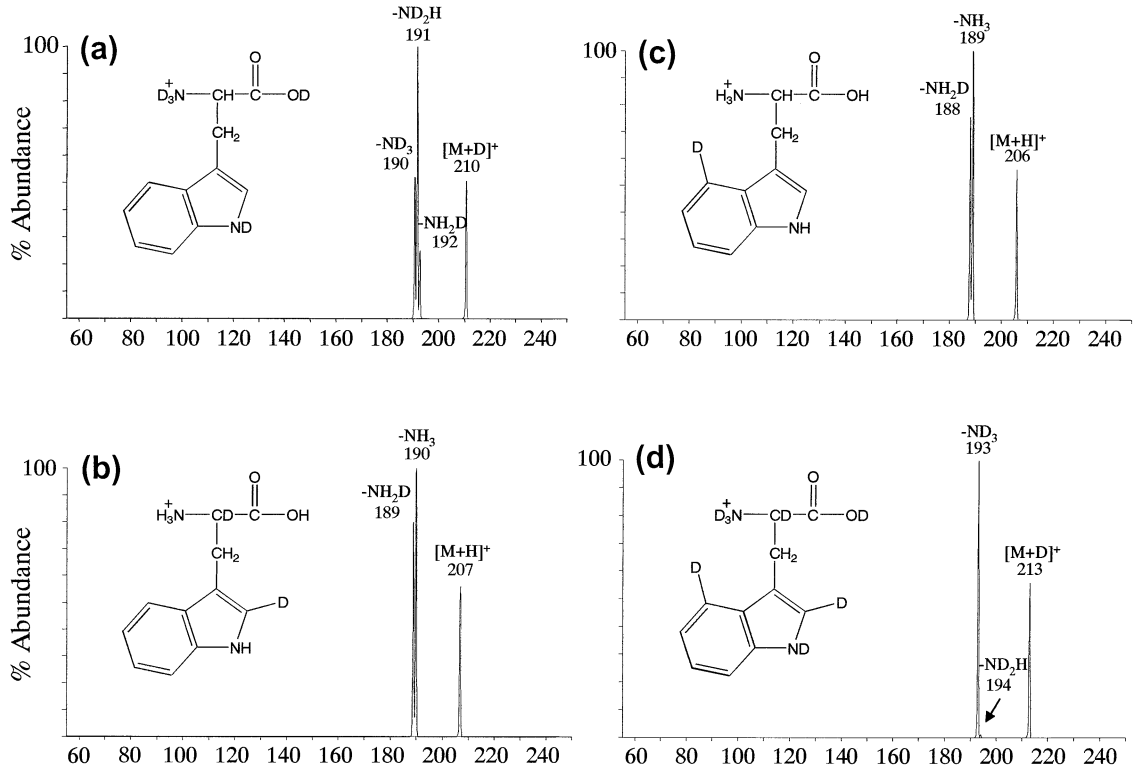


**Figure 2**. CID MS/MS spectra of deuterium labeled tryptophan derivatives. (**a**) $[M + D]^+$ ion of hydrogen–deuterium exchanged tryptophan; (**b**) $[M + H]^+$ ion of C2- and Cα-deuterium substituted tryptophan; (**c**) $[M + H]^+$ ion of C4-deuterium substituted tryptophan; (**d**) $[M + D]^+$ ion of C2-, Cα-, and C4-deuterium substituted and labile hydrogen–deuterium exchanged tryptophan.

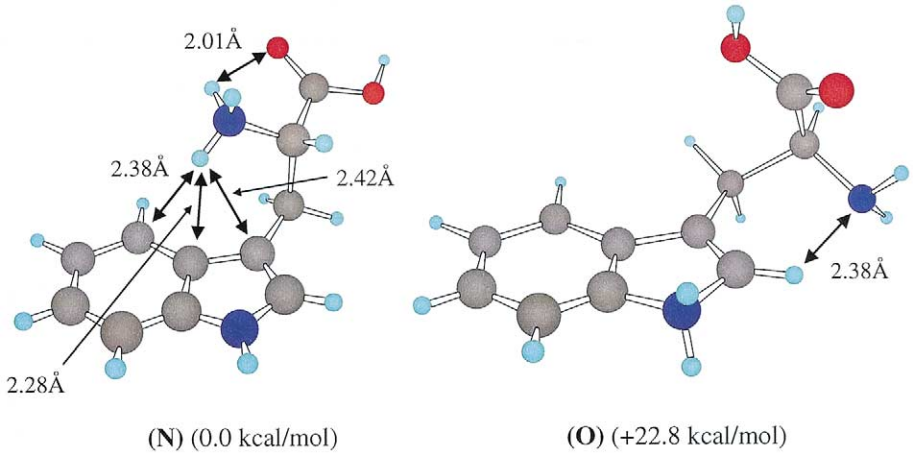


**Figure 3.** B3LYP/6-31G* optimized structures of the lowest energy conformers of tryptophan protonated at the amino nitrogen **N**, and the indole nitrogen **O**.

tryptophan. We have therefore calculated the relative energies of the two isomers of protonated tryptophan, i.e., protonation at the amino nitrogen versus protonation at the indole nitrogen to resolve this issue and to obtain further insights into the mechanisms for the experimentally observed H/D scrambling.

Figure 3 shows the lowest energy isomers for tryptophan that is protonated at the amino nitrogen and indole nitrogen, calculated at the B3LYP/6-31G* level of theory. While it was found that there was little difference in the relative energies (<1.1 kcal/mol) of a number of different low energy rotamers of amino nitrogen protonated tryptophan (the most stable form of tryptophan is that shown as Structure **N**), protonation of the nitrogen atom in the indole nucleus of tryptophan (Structure **O**) was found to be much higher in energy (+22.8 kcal/mol). Note that the stability of the amino protonated global minima is provided by one hydrogen bond between the amino nitrogen and the O atom of the carbonyl group, and another between the amino nitrogen and the $\pi$-electron system of the indole side chain.

## *Computational Studies on Intramolecular Proton Transfer in Protonated Tryptophan*

Given that the preferred site of protonation of tryptophan was predicted to be the amino nitrogen rather than the indole nitrogen, the proposal by Rogalewicz et al. [3e] to explain the experimentally observed scrambling of deuterated tryptophan, via intramolecular proton transfer involving a series of 1,2-hydride shifts from N-indole protonated tryptophan, seems unlikely. Instead, we suggest that intramolecular proton transfer occurs directly from the amino nitrogen to the indole ring. There are six possible intramolecular proton transfers starting from the N-protonated global minimum of tryptophan, that is, proton transfer from the amino nitrogen to the C2, C3, C4, or C9 positions of the indole ring, and proton transfer from the amino nitrogen to the CO or the OH of the carboxylic acid moiety. Of these potential sites for intramolecular proton transfer, only the C2 or C4 positions would allow direct scrambling of labile and non-labile hydrogens.

Figure 4 shows the optimized structures and energies (relative to the global minimum **N**) of species involved in intramolecular proton transfer between the amino nitrogen and the C2 position of the indole side chain, calculated at the B3LYP/6-31G* level of theory. It can be seen that there are two possible pathways for this proton transfer process. The first (Path 1) involves bond rotation around the $C_\alpha$–$C_\beta$ bond to yield Structure **P**, which has an energy +0.9 kcal/mol higher than the global minimum, followed by proton transfer via transition state **TSA** (+11.5 kcal/mol) to form C2-protonated tryptophan (Structure **Q**, +6.8 kcal/mol). It is important to realize that protonation of the C2 position of the indole ring introduces a prochiral center, so that if proton transfer involves a **deuteron**, the ion becomes diastereoisomeric. Consequently, rotation of the amino backbone of the molecule to the opposite face of the indole ring must occur for the **proton** to be intramolecularly transferred back to the amino nitrogen. Species involved in this second intramolecular proton transfer process were calculated, and their optimized structures and relative energies shown in Path 2 of Figure 4. Starting from amino protonated tryptophan, this pathway involves initial bond rotation to yield Structure **N**′ (+0.2 kcal/mol) followed by proton transfer via transition state **TSA**′ (+15.1 kcal/mol), to yield C2-protonated Tryptophan **Q** which has the same structure as that formed by Path 1. Although we have not calculated the transition states for bond rotation connecting the various rotamers of amino protonated tryptophan, we note that previous molecular dynamics calculations on related system suggests that these should be low (≤7 kcal/mol) [23] relative to the proton transfer transition state energies.

The optimized structures and relative energies for species involved in intramolecular proton transfer be-

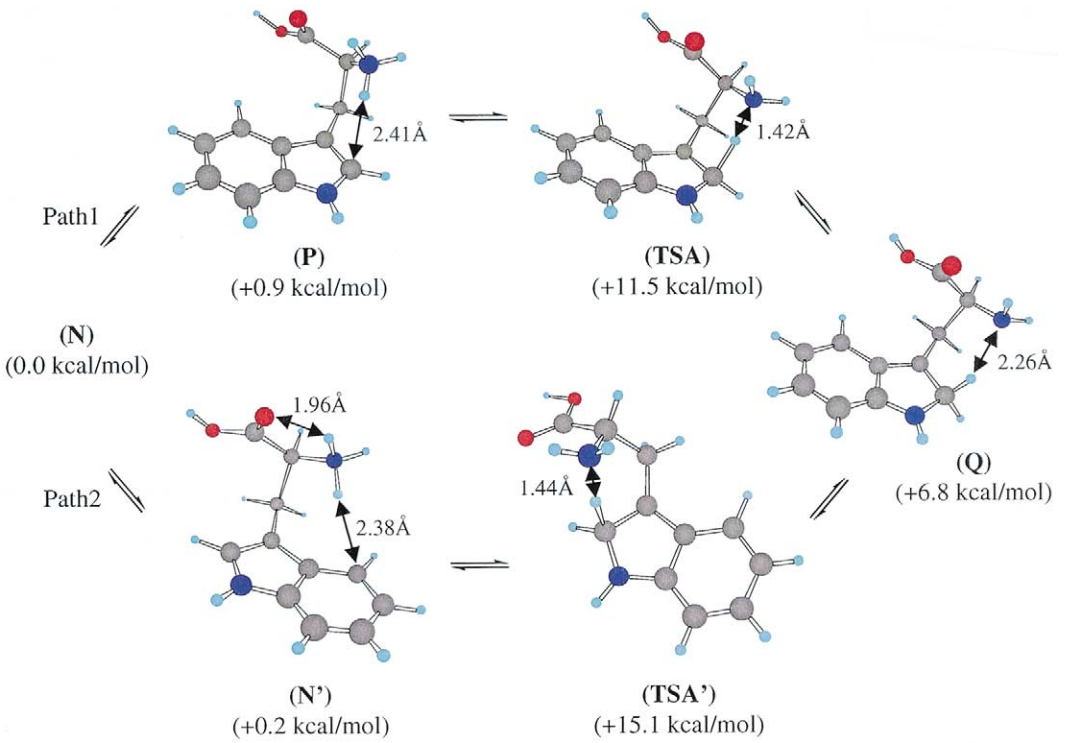


**Figure 4**. B3LYP/6-31G* optimized structures of species associated with intramolecular proton transfer between the amino nitrogen and the C2 position of the indole side chain of protonated tryptophan.

tween the amino nitrogen and C4 of the indole side chain of tryptophan are shown in Figure 5. Similar to that described above for proton transfer to the C2 position, proton transfer to the C4 position can also occur from both faces of the indole ring. In Path 1 of Figure 5, direct intramolecular proton transfer occurs from the global minimum (Structure **N**) via **TSB** (+16.8 kcal/mol) to yield C4-protonated tryptophan (Structure **R**). In Path 2, the same initial bond rotation processes as discussed for Path 2 of Figure 4 for proton transfer to the C2 position takes place to produce Structure **N**′, followed by proton transfer via transition state **TSB**′ (+17.0 kcal/mol) to yield Structure **R**′. Although the optimized structures of C4-protonated tryptophan rotomers **R** and **R**′ are different, a series of low energy bond rotations can easily connect these two structures.

To confirm that intramolecular proton transfer from the amino nitrogen to the C2 and C4 positions of the indole ring are involved in the hydrogen–deuterium scrambling mechanism observed experimentally, we have synthesized regiospecific C2- and C4-deuterium substituted tryptophan derivatives (see experimental data). Figure 2b and 2c show the CID tandem mass spectra of regiospecifically C2- (and $C^{\alpha}$-) deuterium substituted tryptophan, and C4-deuterium substituted tryptophan, respectively, which both show losses of $NH_3$ and $NH_2D$ from the molecular ion. These data clearly demonstrate that both the C2 and C4 positions of the indole ring are involved in the proton scrambling mechanism. The MS/MS data shown in Figure 2b and c, obtained under the same experimental conditions so that the same number of ions and collision energy were used, show that the loss of $NH_2D$ from C2-labeled tryptophan is higher than from C4-labeled tryptophan by approximately 5% relative abundance. This is consistent with the calculated B3LYP/6-31G* transition state energies for the intramolecular proton transfer processes from the amino nitrogen to each of these sites (+15.1 kcal/mol for the C2 proton transfer and +17.0 kcal/mol for the C4 proton transfer). Scheme **4** summarises the proposed process for sequential intramolecular hydrogen–deuterium scrambling from these sites that leads to the loss of $ND_3$, $NHD_2$ and $NH_2D$.

To obtain experimental evidence regarding the potential involvement of protons aside from those at the C2 and C4 indole positions in the scrambling mechanism, a ($N^{\alpha}$,$N^{\alpha}$,O,$\alpha$,1,2,4-$^2H_7$) substituted tryptophan derivative was synthesized by multiple stages of regiospecific deuterium labeling and hydrogen–deuterium exchange and the CID tandem mass spectrum acquired (Figure 2d). While this spectrum shows almost exclusive loss of $ND_3$ from the $[M + D]^+$ ion, the loss of $ND_2H$, indicative of involvement of a proton in addition to those at the C2 or C4 positions, was observed at low (1%) relative abundance. Thus, we have considered other potential mechanisms to account for this observation. A feasible pathway involves a 1,2-hydride shift to and from the C4 and C5 indole positions following intramolecular deuteron–proton transfer to the C4 position from the amino nitrogen. Due to the introduction

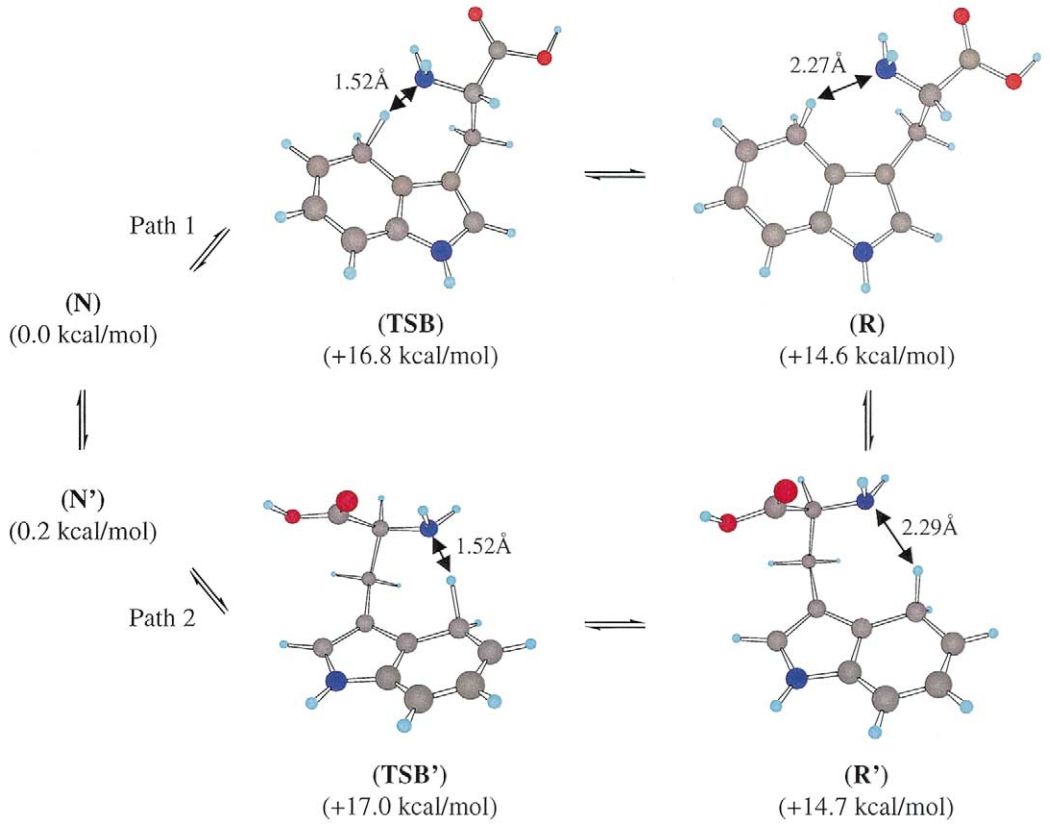


**Figure 5.** B3LYP/6-31G* optimized structures of species associated with intramolecular proton transfer between the amino nitrogen and the C4 position of the indole side chain of protonated tryptophan.

of a prochiral center upon protonation of the C4 position of the indole ring, there are four possible pathways for 1,2-hydride shift between the C4 and C5 positions. i.e., syn- and anti-relative to the face of the indole ring, and front and rear relative to the location of the amino nitrogen. Table 1 shows the relative energies of the transition states for each of these 1,2-hydride shift processes. The average value of the transition state barriers for these 1,2-hydride shifts was determined to be 32.65 kcal/mol, which is considerably higher than those for direct proton transfer between the amino nitrogen and the C2 and C4 indole positions (11.5–17 kcal/mol), and reflects the small relative abundance for the loss of $ND_2H$ compared to $ND_3$ observed in Figure 2d.

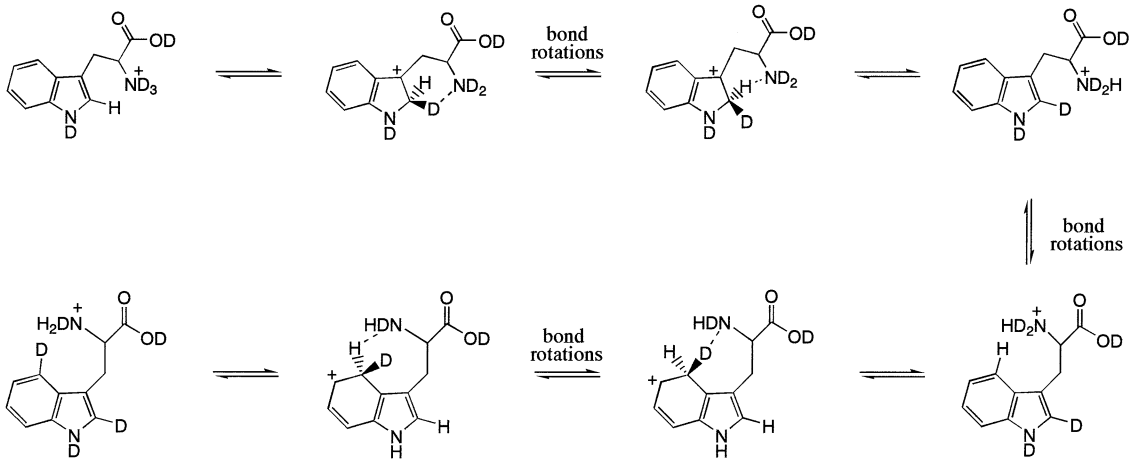


**Scheme 4**

**Table 1.** B3LYP/6-31G* predicted total energies and zero point vibrational energies for various transition states for the 1,2-hydride shifts between positions C4 and C5 of the indole side chain of protonated tryptophan and the associated stable minima

| | Total energies (Hartree) | | Relative energies (kcal/mol) |
|---|---|---|---|
| | B3LYP/6-31G* | ZPVE[a] | |
| C4 protonated front (**R**) | −686.714220 | 0.226815 | 14.6 |
| Transition state-syn | −686.681916 | 0.224094 | 33.2 |
| Transition state-anti | −686.682911 | 0.224086 | 32.6 |
| C5 protonated front | −686.713753 | 0.226978 | 15.0 |
| C4 protonated rear (**R′**) | −686.714051 | 0.226746 | 14.7 |
| Transition state-syn | −686.683707 | 0.224143 | 32.1 |
| Transition state-anti | −686.682633 | 0.224033 | 32.7 |
| C5 protonated rear | −686.713754 | 0.226910 | 15.0 |

[a]Corrected by 0.9806 [19].

## *Reaction Coordinates for the Formation of the $[M + H - NH_3]^+$ Product Ion of Tryptophan*

Given that the experimental results discussed above demonstrate that intramolecular proton scrambling occurs prior to the loss of $NH_3$ (i.e., it is energetically more favorable), we have focused on determining the energies of the isomeric product ion structures formed upon loss of ammonia from protonated tryptophan, and comparing these against the structures proposed by other workers [3, 11]. Table 2 shows the relative energies of the different isomers of the $[M + H - NH_3]^+$ ion, formed by nucleophilic attack from positions 2, 3, 4, 8, and 9 of the indole side chain, calculated at the B3LYP/6-31G* level of theory. These calculations indicate that Structure **K**, formed by nucleophilic attack from the C3 position of the indole side chain, is the lowest energy isomer for the $[M + H - NH_3]^+$ ion. The greater instability of the other isomeric product ion structures can be explained by the geometric strain that is present in the $sp^2$-hybridized carbon at Position 3 of the indole side chain, particularly for Structures **L** and **M**.

Given the significantly greater thermodynamic stability of Structure **K** compared to the other isomeric products, the transition state (**TSC**) for the formation of this ion was calculated at the B3LYP/6-31G* level of theory in order to compare it against those calculated for the hydrogen–deuterium scrambling discussed above. The relative energy of **TSC** (+23.3 kcal/mol relative to the most stable protonated tryptophan conformer **N**), was found to be 6.3 kcal/mol higher than the highest transition state barrier calculated for intramolecular proton transfer and is therefore consistent with the experimental result in which hydrogen–deuterium scrambling occurs in the gas phase prior to $NH_3$ loss (Figure 2a). In a previous section, it was demonstrated that intramolecular proton transfer can occur from both faces of the indole ring. Similarly, it was also possible to displace $NH_3$ by C3-attack from the opposite face of the indole ring to that shown in **TSC**, which yielded a transition state with a similar energy (data not shown). Vibrational frequency analysis confirmed that **TSC** was a transition state with an imaginary frequency of 267.9 $cm^{-1}$ at the B3LYP/6-31G* level of theory, corresponding to the intramolecular displacement of $NH_3$ by the C3 position of the indole ring. The Hessian from the vibrational frequency analysis of **TSC** was used to perform an intrinsic reaction coordinate search, followed by geometry optimization to locate the starting reactant **S**, a conformer of N-protonated tryptophan, and the intermediate **IA**, which is an ion-molecule complex between the spirocyclopropane ion and ammonia. Dissociation of this ion-molecule complex yields **K** plus neutral $NH_3$. The B3LYP/6-31G* optimized structures and energies for this reaction coordinate are shown in Figure 6.

**Table 2.** B3LYP/6-31G* predicted total energies and zero point vibrational energies for various isomeric $[M + H - NH_3]^+$ ions

| | Total energies (Hartree) | | Relative energies (kcal/mol) |
|---|---|---|---|
| | B3LYP/6-31G* | ZPVE[a] | |
| F | −630.115341 | 0.187946 | 19.3 |
| G | −630.130581 | 0.188585 | 10.1 |
| J | −630.115783 | 0.188732 | 19.5 |
| K | −630.146511 | 0.188382 | 0.0 |
| L | −629.993912 | 0.185989 | 94.3 |
| M | −630.080520 | 0.187308 | 40.7 |

[a]Corrected by 0.9806 [19].

The magnitude of the transition state barrier for $NH_3$ loss is expected to be lower than the transition state barrier for loss of the combined elements of $H_2O$ and CO from protonated tryptophan, as indicated by the small relative abundance for $[H_2O + CO]$ loss observed experimentally in Figure 1. As discussed in the introduction, the loss of $H_2O$ and CO requires proton transfer from the thermodynamically favored site of protonation, the amino nitrogen, to the hydroxyl group of the carboxylic acid. We have calculated the energy of this key transition state barrier to be +50.0 kcal/mol (Structure **TSD**) at the B3LYP/6-31G* level of theory. Previous studies on protonated glycine and cysteine yielded values ranging between +30.0 kcal/mol (for protonated cysteine at MP2/6-31G*//HF/6-31G*) and +39.1 kcal/mol (for protonated glycine at B3LYP/6-31G*) [5a, 6] for this transition state. It should be noted

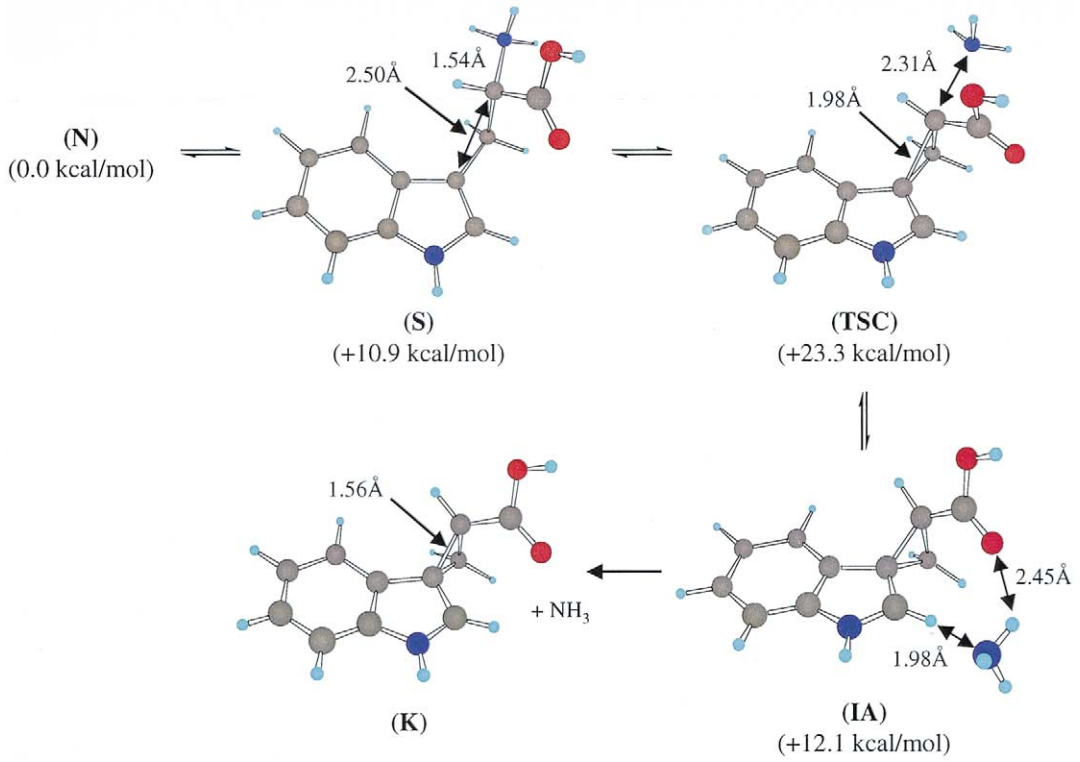


**Figure 6**. B3LYP/6-31G* optimized structures of species associated with the loss of $NH_3$ from protonated tryptophan via nucleophilic attack from the C3 position of the indole side chain.

that rotation about the $C^{\alpha}$–C(carbonyl) bond must occur prior to intramolecular proton transfer from the amino nitrogen to the hydroxyl oxygen. Although we have not calculated the transition state for this bond rotation here, it has been found previously for protonated glycine that the transition state energy for this process was found to be quite low (9.4 kcal/mol at the B3LYP/6-31G* level of theory) [5a]. Thus, the pathway for loss of $NH_3$ in protonated tryptophan is preferred over the combined loss $H_2O$ and CO by 26.7 kcal/mol, a result that is consistent with the experimental data.

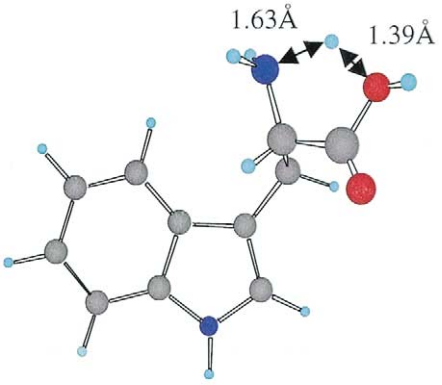


## Conclusions

The use of collisional activation in a quadrupole ion trap, regiospecific deuterium labeling and molecular orbital calculations have proven to be useful in examining the gas-phase reactions of protonated tryptophan. Protonated tryptophan was observed to fragment via the loss of $NH_3$ by nucleophilic attack from the C3 position of the indole side chain. However, under deuterated conditions this loss was preceded by intramolecular proton transfer between the amino nitrogen and the C2 and C4 positions of the indole side chain, resulting in hydrogen–deuterium scrambling. Interestingly, proton transfer to the C2 or C4 position of the indole ring results in the formation of a new chiral center. Therefore, in order for hydrogen–deuterium scrambling to be observed, intramolecular proton transfer from both faces of the indole ring must occur (i.e., delivery of a deuteron from one face and subsequent loss of a proton from the other). In agreement with these experimental data, the results from molecular orbital calculations predict that the activation barriers for these processes follow the order: intramolecular proton transfer $<$ $NH_3$ loss $<$ $H_2O$ + CO loss.

## Acknowledgments

RAJO thanks the Australian Research Council (ARC) for financial support. GER acknowledges the award of an ARC post doctoral fellowship. HL acknowledges the award of an Elizabeth and

Vernon Puzey Postgraduate Research Scholarship. The authors also thank Dr. T. K. Lim for help with NMR, and Ms. Jacinta Watt for carrying out some of the preliminary mass spectrometry experiments.

## References


1. (a) Piraud, M.; Vianey-Saban, C.; Petritis, K.; Elfakir, C.; Steghens, J.-P.; Morla, A.; Bouchu, D. ESI-MS/MS Analysis of Underivatised Amino Acids: A New Tool for the Diagnosis of Inherited Disorders of Amino Acid Metabolism. Fragmentation Study of 79 Molecules of Biological Interest in Positive and Negative Ionization Mode. *Rapid Commun. Mass Spectrom.* **2003,** *17,* 1297–1311. (b) Nagy, K.; Takats, Z.; Pollreisz, F.; Szabo, T.; Vekey, K. Direct Tandem Mass Spectrometric Analysis of Amino Aacids in Dried Blood Spots Without Chemical Derivatization for Neonatal Screening. *Rapid Commun. Mass Spectrom.* **2003,** *17,* 983–990.
2. Klagkou, K.; Pullen, F.; Harrison, M.; Organ, A.; Firth, A.; Langley, G. J. Approaches Towards the Automated Interpretation and Prediction of Electrospray Tandem Mass Spectra of Non-Peptidic Combinatorial Compounds. *Rapid Commun. Mass Spectrom.* **2003,** *17,* 1163−1168.
3. (a) Milne, G. W.; Axenrod, T.; Fales, H. M. Chemical Ionization Mass Spectrometry of Complex Molecules. IV. Amino acids. *J. Am. Chem. Soc.* **1970,** *92,* 5170–5175. (b) Parker, C. D.; Hercules, D. M. Laser Mass Spectra of Simple Aliphatic and Aromatic Amino Acids. *Anal. Chem.* **1985,** *57,* 698–704. (c) Bouchonnet, S.; Denhez, J. P.; Hoppilliard, Y.; Mauriac, C. Is Plasma Desorption Mass Spectrometry Useful for Small-Molecule Analysis? Fragmentations of the Natural α-amino acids. *Anal. Chem.* **1992,** *64,* 743–754. (d) Dookeran, N. N.; Yalcin, T.; Harrison, A. G. Fragmentation Reactions of Protonated α-amino acids.. *J. Mass Spectrom.* **1996,** *31,* 500–508. (e) Rogalewicz, F.; Hoppilliard, Y.; Ohanessian, G. Fragmentation Mechanisms of α-Amino Acids Protonated Under Electrospray Ionization: A Collisional Activation and ab Initio Theoretical Study. *Int. J. Mass Spectrom.* **2000,** *195/196,* 565–590.
4. Harrison, A. G.; Yalcin, T. Proton Mobility in Protonated Amino Acids and Peptides. *Int. J. Mass Spectrom. Ion Processes* **1997,** *165/166,* 339–347.
5. (a) O'Hair, R. A. J.; Broughton, P. S.; Styles, M. L.; Frink, B. T.; Hadad, C. M. The Fragmentation Pathways of Protonated Glycine: A Computational Study. *J. Am. Soc. Mass Spectrom.* **2000,** *11,* 687–696. (b) Rogalewicz, F.; Hoppilliard, Y. Low Energy Fragmentation of Protonated Glycine. An ab Initio Theoretical Study. *Int. J. Mass Spectrom.* **2000,** *199,* 235–252.
6. (a) O'Hair, R. A. J.; Styles, M. L.; Reid, G. E. Role of the Sulfhydryl Group on the Gas Phase Fragmentation Reactions of Protonated Cysteine and Cysteine Containing Peptides. *J. Am. Soc. Mass Spectrom.* **1998,** *9,* 1275–1284. (b) O'Hair, R. A. J.; Reid, G. E. Neighboring group versus cis-Elimination Mechanisms for Side Chain Loss from Protonated Methionine, Methionine Sulfoxide, and Their Peptides Gas Phase Ion Chemistry of Biomolecules. *Eur. Mass Spectrom.* **1999,** *5,* 325–334.
7. (a) Reid, G. E.; Simpson, R. J.; O'Hair, R. A. J. A Mass Spectrometric and ab Initio Study of the Pathways for Dehydration of Simple Glycine and Cysteine-Containing Peptide [M + H]+ Ions. *J. Am. Soc. Mass Spectrom.* **1998,** *9,* 945–956. (b) O'Hair, R. A. J.; Reid, G. E. Does Side Chain Water Loss from Protonated Threonine Yield N-Protonated Dehydroamino-2-Butyric Aacid? *Rapid Commun. Mass Spectrom.* **1998,** *12,* 999–1002. (c) Reid, G. E.; Simpson, R. J.; O'Hair, R. A. J. Probing the Fragmentation Reactions of Protonated Glycine Oligomers via Multistage Mass Spectrometry and Gas Phase Ion Molecule Hydrogen–Deuterium Exchange. *Int. J. Mass Spectrom.* **1999,** *190/191,* 209–230. (d) Reid, G. E.; Simpson, R. J.; O'Hair, R. A. J. Leaving Group and Gas Phase Neighboring Group Effects in the Side Chain Losses from Protonated Sserine and its Derivatives. *J. Am. Soc. Mass Spectrom.* **2000,** *11,* 1047–1060.
8. (a) Zwinselman, J. J.; Nibbering, N. M. M.; Van der Greef, J.; Ten Noever de Brauw, M. C. A Nitrogen-15 Labeling, Field Desorption, and Fast Atom Bombardment Study of Ammonia Loss from Protonated Arginine Molecules. *Org. Mass Spectrom.* **1983,** *18,* 525–529. (b) Van der Greef, J.; Ten Noever de Brauw, M. C.; Zwinselman, J. J.; Nibbering, N. M. M. A Fast Atom Bombardment Study of Methionine in Combination with Deuterium Labeling. *Org. Mass Spectrom.* **1982,** *17,* 274–276.
9. Dongre, A. R.; Jones, J. L.; Somogyi, A.; Wysocki, V. H. Influence of Peptide Composition, Gas-Phase Basicity, and Chemical Modification on Fragmentation Efficiency: Evidence for the Mobile Proton Model. *J. Am. Chem. Soc.* **1996,** *118(8365),* 8374.
10. O'Hair, R. A. J. The Role of Nucleophile–Electrophile Interactions in the Unimolecular and Bimolecular Gas-Phase Ion Chemistry of Peptides and Related Systems. *J. Mass Spectrom.* **2000,** *35,* 1377−1381.
11. Prokai, L.; Prokai-Tatrai, K.; Pop, E.; Bodor, N.; Lango, J.; Roboz, J. Fast Atom Bombardment and Tandem Mass Spectrometry of Quaternary Pyridinium Salt-Type Tryptophan Derivatives. *Org. Mass Spectrom.* **1993,** *28,* 707−715.
12. (a) Shoeib, T.; Cunje, A.; Hopkinson, A. C.; Siu, K. W. M. Gas-Phase Fragmentation of the Ag+-Phenylalanine Complex: Cation-p Interactions and Rradical Cation Formation. *J. Am. Soc. Mass Spectrom.* **2002,** *13,* 408–416. (b) Johansen, J. E.; Christie, B. D.; Rapoport, H. Iminium Salts from α-Amino Acid Decarbonylation. Application to the Synthesis of Octahydroindolo[2,3-α]Quinolizines. *J. Org. Chem.* **1981,** *46,* 4914–4920.
13. (a) Saito, I.; Sugiyama, H.; Yamamoto, A.; Muramatsu, S.; Matsuura, T. Photochemical Hydrogen–Deuterium Exchange Reaction of Tryptophan. The Role of Nonradiative Decay of Singlet Tryptophan. *J. Am. Chem. Soc.* **1984,** *106,* 4286–4287. (b) Saito, I.; Muramatsu, S.; Sugiyama, H.; Yamamoto, A.; Matsuura, T. Regio-Controlled Hydrogen–Deuterium Exchange of Biologically Important Indoles Under UV Irradiation. *Tetrahedron Lett* **1985,** *26,* 5891–5894. (c) Shizuka, H.; Serizawa, M.; Shimo, T.; Saito, I.; Matsuura, T. Fluorescence-Quenching Mechanism of Tryptophan. Remarkably Efficient Internal Proton-Induced Quenching and Charge-Transfer Quenching. *J. Am. Chem. Soc.* **1988,** *110,* 1930–1934. (d) Cozens, F.; McClelland, R. A.; Steenken, S. Flash Photolysis Observation and Lifetimes of the Cation Intermediates in the Intramolecular Photoprotonation of Tryptamine, Tryptophan, and their N-Methyl Derivatives. *Tetrahedron Lett.* **1992,** *33,* 173–176.
14. Griffiths, D. V.; Feeney, J.; Roberts, G. C. K.; Burgen, A. S. V. Preparation of Selectively Deuterated Aromatic Amino Acids for Use in Proton NMR Studies of Proteins. *Biochim. Biophys. Acta* **1976,** *446,* 479–485.
15. Hehre, W. J.; Radom, L.; Schleyer, P.v.R.; Pople, J. A. Ab Initio Molecular Orbital Theory; Wiley Interscience: New York, 1986, pp. 79–82.
16. Schmidt, M. W.; Baldridge, K. K.; Boatz, J. A.; Elbert, S. T.; Gordon, M. S.; Jensen, J. H.; Koseki, S.; Matsunaga, N.; Nguyen, K. A.; et al. General Atomic and Molecular Electronic Structure System. *J. Comput. Chem.* **1993,** *14,* 1347–1363.
17. Frisch, M. J.; Trucks, G. W.; Schlegel, H. B.; Scuseria, G. E.; Robb, M. A.; Cheeseman, J. R.; Zakrzewski, V. G.; Montgomery, J. A.; Stratmann, R. E.; Burant, J. C.; Dapprich, S.; Millam, J. M.; Daniels, A. D.; Kudin, K. N.; Strain, M. C.; Farkas, O.; Tomasi, J.; Barone, V.; Cossi, M.; Cammi, R.; Mennucci, B.; Pomelli, C.; Adamo, C.; Clifford, S.; Ochterski, J.; Petersson, G. A.; Ayala, P. Y.; Cui, Q.; Morokuma, K.; Malick, D. K.; Rabuck, A. D.;

Raghavachari, K.; Foresman, J. B.; Cioslowski, J.; Ortiz, J. V.; Stefanov, B. B.; Liu, G.; Liashenko, A.; Piskorz, P.; Komaromi, I.; Gomperts, R.; Martin, R. L.; Fox, D. J.; Keith, T.; Al-Laham, M. A.; Peng, C. Y.; Nanayakkara, A.; Gonzalez, C.; Challacombe, M.; Gill, P. M. W.; Johnson, B. G.; Chen, W.; Wong, M. W.; Andres, J. L.; Head-Gordon, M.; Replogle, E. S.; Pople, J. A; Schmidt, M. W.; Baldridge, E. K. K.; Boatz, J. A.; Elbert, S. T.; Gordon, M. S.; Jensen, J. H.; Koseki, S.; Matsunaga, N.; Nguyen, K. A.; Su, S. J.; Windus, T. L.; DuPuis, M.; Montgomery, J. A.. Gaussian 98 Rev. A.7; Gaussian, Inc.: Pittsburgh, PA, 1998.

18. Schaftenaar, G.; Noordik, J. H. Molden: A Pre- and Post-Processing Program for Molecular and Electronic Structures. *J. Comput. Aid. Mol. Design* **2000,** *14,* 123–134.
19. Scott, A. P.; Radom, L. Harmonic Vibrational Frequencies: An Evaluation of Hartree-Fock, Moller-Plesset, Quadratic Configuration Interaction, Density Functional Theory, and Semiempirical Scale Factors. *J. Phys. Chem.* **1996,** *100,* 16502–16513.
20. (a) Norton, R. S.; Bradbury, J. H. Kinetics of Hydrogen–Deuterium Exchange of Tryptophan and Tryptophan Peptides in Deutero-Trifluoroacetic Acid Using Proton Magnetic Resonance Spectroscopy. *Mol. Cell. Biochem.* **1976,** *12,* 103–111. (b) Bak, B.; Dambmann, C.; Nicolaisen, F. Hydrogen–Deuterium Exchange in Tryptophan. *Acta. Chem. Scand.* **1967,** *21,* 1674–1675.
21. Maksic, Z. B.; Kovacevic, B. Towards the Absolute Proton Affinities of 20 $\alpha$-Amino Acids. *Chem. Phys. Lett.* **1999,** *307,* 497–504.
22. Mirza, S. P.; Prabhakar, S.; Vairamani, M. Estimation of Proton Affinity of Proline and Tryptophan Under Electrospray Ionization Conditions Uusing the Extended Kinetic Method. *Rapid Commun. Mass Spectrom.* **2001,** *15,* 957–962.
23. Gordon, H. L.; Jarrell, H. C.; Szabo, A. G.; Willis, K. J.; Somorjai, R. L. Molecular Dynamics Simulations of the Conformational Dynamics of Tryptophan. *J. Phys. Chem.* **1992,** *96,* 1915–1921.